J. Phycol. **45,** 1106–1115 (2009)

DOI: 10.1111/j.1529-8817.2009.00740.x

CELL CYCLE AND CELL MORTALITY OF *ALEXANDRIUM MINUTUM* (DINOPHYCEAE) UNDER SMALL-SCALE TURBULENCE CONDITIONS[1]

Gisela Llaveria,[2,3] *Rosa Isabel Figueroa, Esther Garcés, and Elisa Berdalet*[3]

Institut de Ciències del Mar, CSIC, Passeig Marítim de la Barceloneta, 37-49, E-08003 Barcelona, Spain

Decreased net population growth rates and cellular abundances have been observed in dinoflagellate species exposed to small-scale turbulence. Here, we investigated whether these effects were caused by alterations in the cell cycle and/or by cell mortality and, in turn, whether these two mechanisms depended on the duration of exposure to turbulence. The study was conducted on the toxic dinoflagellate *Alexandrium minutum* Halim, with the same experimental design and setup used in previous studies to allow direct comparison among results. A combination of microscopy and Coulter Counter measurements allowed us to detect cell mortality, based on the biovolume of broken cells and thecae. The turbulence applied during the exponential growth phase caused an immediate transitory arrest in the G2/M phase, but significant mortality did not occur. This finding suggests that high intensities of small-scale turbulence can alter the cell division, likely affecting the correct chromosome segregation during the dinomitosis. When shaking persisted for >4 d, mortality signals and presence of anomalously swollen cells appeared, hinting at the activation of mechanisms that induce programmed cell death. Our study suggests that the sensitivity of dinoflagellates to turbulence may drive these organisms to find the most favorable (calm) conditions to complete their division cycle.

Key index words: ***Alexandrium minutum*****; cell cycle; Coulter Counter; dinoflagellates; flow cytometry; G2/Mitosis; mortality; small-scale turbulence**

Abbreviations: **ε, turbulent kinetic energy dissipation rate; μ, net exponential growth rate**

Understanding of harmful algal bloom (HAB) dynamics requires evaluating how different environmental factors influence the physiology and biology of the involved organisms. In the case of dinoflagellates, a phytoplankton group that includes several HAB-producing species, small-scale turbulence appears to be a key physical factor that can affect particular aspects of their biology (reviews by Peters and Marrasé 2000, Berdalet and Estrada 2005).

Several field studies have documented the capacity of dinoflagellates to adjust their motion and position to the turbulence intensity (Eppley et al. 1968, Margalef et al. 1979, Sullivan et al. 2003). Their swimming behavior, combined with certain circulation features (convergences, relaxation of upwelling), may favor accumulation in relatively calmed and stratified environments (Wyatt and Horwood 1973, Margalef 1978, Smayda and Reynolds 2001) in a broad range of scenarios (coastal embayments, estuaries and retention areas, such as eddies in shelf waters). Furthermore, in 72% of a number of experimental studies conducted on this phytoplankton group (listed in Berdalet et al. 2007), turbulence caused a decrease in the net growth rate and/or low cellular abundances and physiological alterations, such as changes in swimming behavior (Estrada et al. 1987, Thomas and Gibson 1990, Chen et al. 1998, Karp-Boss et al. 2000, Berdalet et al. 2007), cell morphology (Zirbel et al. 2000), increase of cell size, RNA and DNA cell content (Berdalet 1992, Yeung and Wong 2003, Berdalet et al. 2007), modified cellular toxin concentration (Juhl et al. 2001, Bolli et al. 2007), bioluminescence stimulation (Anderson et al. 1988, Latz et al. 1994, Latz and Rohr 1999), and encystment inhibition (Anderson and Lindquist 1985, Tynan 1993, Smith and Persson 2005, Bolli et al. 2007). These alterations suggest an interference of small-scale turbulence with cell division and life-cycle processes. An inhibition of cell division would result in the often reported decrease in net growth rate and cellular abundances, although a certain degree (simultaneous or not) of cell mortality can also occur (e.g., Pollingher and Zemel 1981, Thomas and Gibson 1990, Berdalet 1992, Juhl et al. 2000, Sullivan and Swift 2003). However, to discriminate whether turbulence caused the inhibition of cell division and/or cell death is difficult, mainly due to methodological limitations. To differentiate between these two processes could contribute to the comprehension of the underlying mechanisms of the dinoflagellate response to small-scale turbulence. Cell division inhibition can be caused by an alteration of the cell cycle, implying a total or partial arrest in a particular phase (Murray and Hunt 1993). For instance, the decrease in cell

[1]Received 31 July 2008. Accepted 6 May 2009.
[2]Author for correspondence: e-mail llaveria@cmima.csic.es.
[3]These authors contributed equally to this work.

division in *Lingulodinium polyedrum* cultures was associated with a lengthening of the G1 (gap followed by DNA synthesis, or S phase) or of G2 (gap preceded by S phase) phases depending on the duration and intensity of flow shear generated by a Couette system or by a reciprocal shaker (Juhl and Latz 2002). Yeung and Wong (2003) reported a transient cell-cycle arrest in the G1 phase of *Heterocapsa triquetra* and *Crypthecodinium cohnii* cultures exposed to continuous orbital shaking. Flow cytometry was used in the two studies to characterize the effect of turbulence on the cell cycle. A temporary arrest in the G2 phase of the cell cycle, and thus no progression through mitosis (M phase), was suggested to occur in *Akashiwo sanguinea* (Berdalet 1992), *Prorocentrum triestinum*, and *A. minutum* (Berdalet et al. 2007) when exposed to orbital shaking. In these three species, low cell abundances and net growth rates under turbulence were accompanied by increases in both cellular DNA concentration (up to 10-, 5.3-, and 1.8-fold, respectively, relative to controls) and cell size (up to 1.5, 2.5, and 1.4 times relative to controls, respectively). In these two studies, DNA was estimated biochemically, but unfortunately, detailed cell-cycle observations that could have identified a certain cell-cycle alteration were not performed.

Decreased or negative net growth rates caused by different experimental turbulence conditions were associated with cell death based on different observations. Damaged or broken cells were observed (although mortality rates were not quantified) in the studies by Tuttle and Loeblich (1975), Galleron (1976), White (1976), Thomas and Gibson (1990), and Berdalet (1992). Juhl and Latz (2002) assessed the impact of turbulence in *L. polyedrum* through the comparison of the percentage of intact and disrupted cells and of cells with damaged membranes in sheared and in undisturbed cultures. Furthermore, based on the similarity or discrepancy between potential growth rates estimated by flow cytometry and the net growth rates estimated by microscopic cell enumeration, these authors discriminated between inhibition of the cell cycle and mortality. By this approach, they noted that the mechanism by which shear stress generated by Couette flow inhibited the net growth rate of *L. polyedrum* depended on shear stress levels and growth conditions. They hypothesized that natural turbulence levels may cause inhibition of cell division, with a subsequent delay in bloom development. In contrast, the shear-induced mortality observed during the stationary phase of their cultures suggested that high shear levels would contribute to bloom termination. These authors concluded that it was difficult to ascertain whether other species different from *L. polyedrum* would have had the same response. As it is known (Berdalet and Estrada 1993, Sullivan and Swift 2003), the response of dinoflagellates to turbulence is highly species specific.

In our present study, we investigated whether cell-cycle alterations and cell mortality induced by turbulence were involved in the decrease in net growth rate and cellular abundances of another dinoflagellate, *A. minutum* (Berdalet et al. 2007, Bolli et al. 2007). This organism is a paralytic shellfish poisoning (PSP) toxin producer species that proliferates in coastal areas including the Mediterranean ones (Halim 1960, Delgado et al. 1990, Honsell et al. 1995, Vila et al. 2001).

In our previous studies with *A. minutum*, we had shown that turbulence generated by an orbital shaker resulted in low net growth rate, low cellular abundances, low toxin (GTX1 + 4, C1 + 2) content, increase in cell size and DNA concentration, and inhibition of ecdysal cyst production (Berdalet et al. 2007, Bolli et al. 2007). The observed responses were detected after 1–2 d of exposure to turbulence, and they suggested that turbulence could have very early effects on the cell. However, it was not possible to specify whether changes had occurred at the level of cell division or due to mortality, and which mechanism could operate first.

In the present study, we explored whether turbulence induced short-term changes in the cell cycle of *A. minutum*. Cultures were intensively sampled over a 24 h period after 2 d of exposure to the turbulent regime, and changes in DNA content of the cells population were examined using flow cytometry. Thereafter, DNA content was measured daily to track the possible cell-cycle alterations over a long-term exposure to turbulence. Additionally, particle size spectra were characterized using a Coulter Counter to obtain an indicator of morphological alterations and of cell mortality due to the exposure to turbulence. In particular, changes in the biovolume of broken theca were used as an indirect and rather qualitative indication of cell death (see Materials and Methods). We based our approach on Knoechel and Kalff (1978) who estimated mortality rates in diatoms by counting the number of empty frustules, but we previously tested all possible limitations before applying it (see Materials and Methods). Unfortunately, more recent approaches based on differential cell staining of live and dead cells (Veldhuis et al. 1997, 2001, Jochem 1999, Garvey et al. 2007) did not provide consistent results to estimate mortality in our preliminary tests with *A. minutum*. Experimental conditions and setup (including the orbital shaker) were analogous to those utilized in previous experiments (Berdalet 1992, Berdalet et al. 2007, Bolli et al. 2007) to allow direct comparison among studies.

MATERIALS AND METHODS

Cultures. The *A. minutum* clonal strain employed in this study was VGO 651, kindly provided by the Vigo Oceanographic Center (Spain). A nonaxenic unialgal culture was maintained in exponential phase in L1 seawater enriched media (Guillard and Hargraves 1993) without silica addition.

Mediterranean Sea water was collected at 5 m depth, adjusted to 31 psu by the addition of double-distilled water, and autoclaved. Nutrient stocks were sterilized separately and added to the seawater under sterile conditions 24 h after autoclaving. Stock and experimental cultures were grown in a culture chamber at 20 ± 1°C on a 12:12 light:dark (L:D) cycle (light period starting at 17:00 h local time) and 110 μmol photons · m^{-2} · s^{-1} irradiance provided by the combination of Gyrolux (58 W, Sylvania, Erlangen, Germany) and cool-white (58 W, Philips, Eindhoven, the Netherlands) fluorescent tubes (in a 1:1 proportion).

Experimental setup. Four 4 L Florence flasks (Pyrex spherical flasks with flat bottom) containing 3 L of medium were inoculated with the same initial cell concentration (334 ± 14 cells · mL^{-1}). On day 5 following inoculation, during the early exponential phase (as repeatedly tested previously), all cultures were kept in the dark for 48 h in order to synchronize the cultures with the diel cycle (Taroncher-Oldenburg et al. 1997, Figueroa et al. 2007). By this treatment, >95% of the cells would be at G1, and cell division of most of them would occur synchronously with the diel cycle for at least 3 d. Until this moment, all four experimental flasks had been subjected to the same conditions, and they were considered as replicates. On day 7 at 0:00 h local time (corresponding to 7 h after onset of light and 5 h before the dark period), just after sampling, two flasks (thereafter referred to as *Turbulent*) were randomly chosen to be subjected to continuous turbulence, while two flasks were kept still as controls (thereafter referred to as *Still*). Two days after the start of turbulence, on day 9, samples were taken at regular time intervals of 2 h during 24 h to test the early effect of turbulence on the cell cycle by flow cytometric analysis (FACScalibur bench machine; Becton and Dickinson, San Jose, CA, USA). Thereafter, samplings were performed once per day until the end of the experiment to track the long-term effect of turbulence. Samples for cell counts, measurement of cell size, and flow cytometric analysis were taken daily at 0:00 h. We expected that at this time of the L:D cycle most populations were in G1 (Figueroa et al. 2007) unless modified by turbulence. To minimize disturbance of the *Still* flasks when sampling, they were carefully and gently swirled.

Turbulence setup. Turbulence was generated using an orbital shaker (AOS, SBS, Rubí, Spain) operating at 120 rpm with a displacement of 30 mm. This corresponds to an average turbulent kinetic energy dissipation rate, ε, of 27 $cm^2 \cdot s^{-3}$ (2.7×10^{-3} W · kg^{-1}, Bolli et al. 2007).

Measurements. Cell abundances (a daily sample from each experimental flask) were estimated by microscopy (Axiovert 35; Zeiss, Oberkochen, Germany) with Sedgewick-Rafter counting cell slides (Ref. 02B00417, PYSER-SGI, Edenbridge, UK) after fixation with Lugol's iodine solution. A minimum of 400 cells were counted. Net exponential growth rates (μ, d^{-1}, as defined by Guillard 1973) were calculated as the slope of the regression line of $\ln(N)$ versus time (t), where N was the estimated cell abundance by microscopic counting.

Flow cytometric DNA analyses were performed following the method described by Figueroa et al. (2006, 2007). From each experimental flask, a 45 mL sample taken in every sampling time was fixed in 1% paraformaldehyde for 10 min at room temperature and washed with pH 7 PBS (Sigma-Aldrich, St. Louis, MO, USA, #P4417). After centrifugation (3,893*g*, 20 min; Sigma 3-16K, Fisher Bioblock Scientific, Illkirch, France) the pellet was resuspended in 3 mL cold methanol and stored for 12 h at 4°C to extract chl. Cells were washed twice in PBS and resuspended in staining solution (PBS, 3 μg · mL^{-1} propidium iodine and 1.1 μg · mL^{-1} RNAase) for at least 2 h before analysis. We used a Becton and Dickinson FACScalibur bench machine with a laser emitting at 488 nm and detection of the propidium iodide fluorescence at 617 nm. Samples were run at low speed (~18 μL · min^{-1}), and data were acquired in linear and log mode until ~10,000 events had been recorded. To each sample, 10 μL of a 10^6 particles · mL^{-1} solution of yellow-green 0.92 μm Polysciences latex beads (Polysciences, Inc., Warrington, PA, USA) were added as internal standard. ModFit LT (Verity Software House, Topsham, ME, USA), a curve-fitting program commonly used for the treatment of dinoflagellate flow cytometry data (Taroncher-Oldenburg et al. 1997, Pan and Cembella 1998, Peperzak et al. 1998, Yeung and Wong 2003, Figueroa et al. 2006, 2007), was used to determine the distribution of the DNA fluorescence of the population, computing peaks, their ratios, and coefficients of variation (CVs) of the histogram obtained in this way per each sample. To compare the trends of the different treatments concerning the cell-cycle pattern, percentages of cells in G1, S, and G2/M phases were adjusted to 5 degree polynomial curves. The duration of S and G2/M phases were estimated as a function of the respective adjusted curve peak values and of the distance between them (Carpenter and Chang 1988).

In vivo measurements of the population size spectrum were performed immediately after sampling using a Multisizer 3 Coulter Counter (Beckman Coulter, Fullerton, CA, USA). This instrument is provided with a 100 μm aperture tube, with an effective particle-size range of 2–60 μm (equivalent spherical diameter) and a 300 channel particle-size analyzer. The Coulter Counter measurements, in combination with microscopy observations (Axiovert 35; Zeiss), were used to identify cellular changes and to estimate cell mortality as follows. According to Figueroa et al. 2007, the common vegetative forms fall in the range of 13 to 25 μm in diameter. Microscopic observations, however, revealed that cells undergoing premitosis and mitosis (G2/M, during the exponential phase of the cultures) or not (from the stationary phase) and aberrant forms (especially in the stationary phase of the turbulent treatment) were >25 μm in diameter. In this range, we did not expect contribution by cells originated after sexual fusion, because this species is heterothallic (not self-compatible, Figueroa et al. 2007) and because we used a clonal strain. This broad category of cells, hereafter referred to as ''large cells,'' contributed to the 25.13 to 30.17 μm (equivalent spherical diameter) size range of the in vivo spectra identified by the Coulter Counter. Indeed, the abundance of large cells estimated by microscopy was significantly correlated with the particle numbers in the 25.13–30.17 μm range measured by the Coulter Counter ($r^2 = 0.896$; $P = 0.001$, $n = 7$; Fig. 1a). The changes over time in this large cells category allowed us to confirm trends suggested by flow cytometry (e.g., increase in the G2/M fraction of the population) or by microscopy (e.g., increase in aberrant forms during the stationary phase), linked to the experimental treatments (see Results, Fig. 4).

To estimate cell mortality, we hypothesized that empty and broken thecae and fragments of cells would contribute to the particles estimated by the Coulter Counter in the size fraction <13 μm. Thus, a proxy for mortality would be the ratio between the volume of particles in the size range <13 μm (contributed mainly by thecae plus fragments) and the volume corresponding to vegetative cells estimated in the 13–25 μm size range. This proxy requires that, apart from mortality, there are no other mechanisms that naturally produce empty theca, such as ecdysis (the process linked to cyst production by which a cell sheds its theca and emerges as a nonmotile cell surrounded by a pellicle) or losses of the mother theca during mitosis. Unlike other dinoflagellates, *A. minutum* does not eliminate the theca when it divides (Figueroa et al. 2007), and the chosen VGO 651 clone has very low ecdysal cyst production (<6%, G. Llaveria, unpublished data) under our culture conditions. To validate the estimations of the thecae abundances by the Coulter Counter, different samples collected during the experiment were stained with Calcofluor White M2R (#F3543, Fluorescent Brightener 28, Sigma, St. Louis, MO, USA) to visualize the

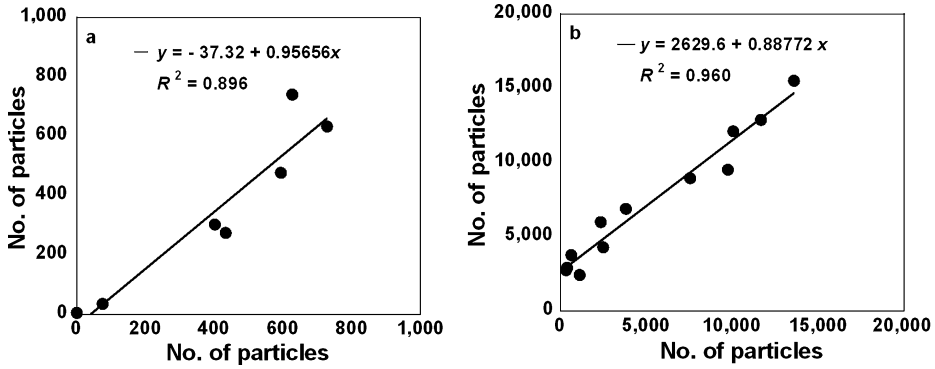

FIG. 1. Comparisons between the estimations of the number of particles by Coulter Counter (*y*-axis) and microscopy counts (*x*-axis). (a) Comparison of the particles contributing to the 25.13–30.17 μm size range estimated by the Coulter Counter and the abundance of large cells including premitotic, mitotic, and aberrant cells. (b) Comparison of the number of particles contributing to the 7–13.05 μm size range estimated by Coulter Counter and abundances of broken thecae visualized by Calcofluor and microscopy. The regression lines obtained in each comparison and their degree of correlation are indicated inside each graph.

thecae by microscopy (Fritz and Triemer 1985). A positive and significant relationship ($r^2 = 0.960$; $P = 0.000$, $n = 12$) was obtained between the abundances of broken thecae estimated microscopically and the number of particles contributing to the 7 to 13.05 μm range estimated by the Coulter Counter (Fig. 1b). The number of particles in this size range could increase by the breakage of the empty theca into smaller pieces (especially in the turbulent treatment), and not only for an increase in the number of empty theca linked to cell death, while the volume would remain constant. Thus, biovolume was chosen as a more conservative estimation for mortality. The ratio (expressed in %) of the biovolume ($\mu m^3 \cdot L^{-1}$) of the 7–13 μm to the 13–25 μm size fraction was used as a proxy for mortality.

Statistical analyses were performed using Systat 11 for PC (Systat Software Inc., Point Richmond, CA, USA). Comparison of treatments over time for the different parameters was done using the nonparametric Kruskal–Wallis test (Motulsky 2003). Net growth rates were compared by testing for the heterogeneity of slopes (analysis of covariance).

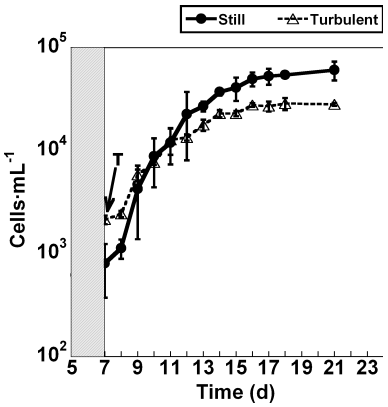

FIG. 2. Temporal changes in cell abundances in the two treatments, *Still* and *Turbulent*, estimated by microscopy. Data points and vertical bars are averages and standard deviations, respectively ($n = 2$). The shaded area represents the synchronization period during days 5 to 7. ''T'' indicates the beginning of turbulence in the corresponding flasks on day 7.

RESULTS

Development of the cultures. Although the four flasks were inoculated with the same cell concentration (334 ± 14 cel $\cdot$ mL^{-1}), at the end of the synchronization period on day 7, cell densities differed among them (range 500–2,277 cells $\cdot$ mL^{-1}, Fig. 2). By chance, the two flasks that had the lower cell numbers were the ones that had been labeled as *Still* at the beginning of the experiment. Although the 48 h dark period had some kind of negative effect on these two cultures (see ''Mortality'' section), cell numbers recovered rapidly afterward, indicating that the synchronization period did not drastically affect the capacity of the population to proliferate.

The *Still* populations grew exponentially from days 8 to 12, were in a transition phase from days 12 to 17, and entered into the stationary phase thereafter. The *Turbulent* cultures ended the exponential phase on day 11, 1 d earlier than the *Still* ones, although the transition phase lasted also for 5 d, until day 16, when they entered into the stationary phase. The exponential net growth rate of the *Turbulent* cultures (0.52 ± 0.06 d^{-1}, $r^2 = 0.917$) was significantly lower ($P = 0.005$, $n = 18$), being 75% of the growth rate observed in *Still* cultures (0.69 ± 0.11 d^{-1}, $r^2 = 0.824$). At the end of the experiment, from days 16 to 21, the final cell abundance of the *Turbulent* treatment ($27{,}852 \pm 3{,}461$ cells $\cdot$ mL^{-1}) was ~51% of the cell abundance in *Still* cultures ($54{,}333 \pm 14{,}917$ cells $\cdot$ mL^{-1}) (Mann–Whitney *U*-test = 64.0; $P = 0.001$, $n = 16$).

Short-term effects of turbulence on cell cycle. At the end of the synchronization period (on day 7) and at 0:00 h, the histograms of the DNA content of the four cultures (all kept under the same still conditions until then) had well-defined peaks with small coefficients of variation, $\sim 5.6 \pm 0.2\%$ (average ± standard error of the mean, $n = 4$, not shown). All the cultures were well phased to the

L:D cycle (Fig. 3, a, c, and e); data corresponded to day 7 at 0:00 h because at that time of the day ~95.2 ± 0.4% of the populations were in G1 phase, and a negligible fraction of cells were in G2/M. Thus, turbulence was applied in cultures with synchronized cell cycle. The synchronization remained in the *Still* cultures during the intensive 24 h sampling from days 9 to 10 (Fig. 3, b, d, and f; Table 1). During this period, the percentage of cells in G1 increased from 67% to 94%, between 10:30 h and 22:00 h. The fraction of the population entering S phase increased from 2% to 16% from 19:30 h (2.5 h after the end of the dark period) to 7:30 h, considering two consecutive days. Finally, from 1:00 h to 12:00 h, the percentage of cells in the G2/M phase increased by 29%. Under these conditions, the durations of the S and G2/M phases were 3 h 20 min and 5 h 40 min, respectively.

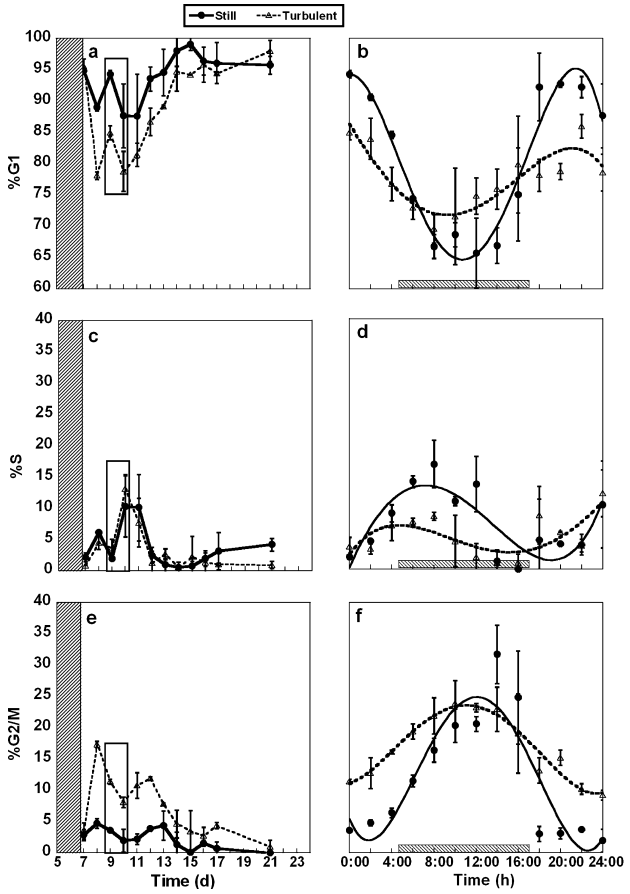

FIG. 3. Left panels: temporal changes at 0:00 h in the percentage of cells in G1 (a), S (c), and G2/M (e) phases in the two treatments, *Still* and *Turbulent*, over the whole experiment. Right panels: percentage of cells in G1 (b), S (d), and G2/M (f) phases in the cultures exposed to these two treatments during a 24 h diel cell cycle, from days 9 to 10. Data points and vertical bars are averages and standard deviations, respectively ($n = 2$). In (a), (c), and (e), the rectangles show the period of the intensive cell-cycle study illustrated in (b), (d), and (f). In (b), (d), and (f), the shaded areas represent the dark period during the diel cycle. Adjusted curves are polynomial equations describing the G1 phase, with $r^2 = 0.950$ and 0.829 for the *Still* and the *Turbulent* treatments, respectively; analogously for the description of the S ($r^2 = 0.809$ and 0.507) and for the G2/M ($r^2 = 0.820$ and 0.955) phases.

At 0:00 h on day 9 (i.e., after 2 d under turbulence), the percentage of cells in G1 and G2/M was clearly lower and higher, respectively, than the corresponding numbers in the *Still* treatments (Fig. 3, a, b, e, and f). The intensive sampling during days 9–10 showed that the cell-cycle pattern observed in the *Still* treatments had been modified by 2 d exposure to turbulence (Fig. 3, b, d, and f). Under agitation, the adjusted curves that described the G1, S, and G2/M phases had smaller amplitudes than the ones corresponding to the *Still* cultures, and the peaks and valleys were smoothed. As specified in Table 1, the timing of the cell-cycle phases with the L:D cycle in the shaken cultures changed compared to the *Still* ones. Furthermore, the percentage of the population that entered the G1 and the S phases was lower in the *Turbulent* than in the *Still* conditions. However, cells with double DNA content (G2/M phase) were observed along the whole diel cycle in the *Turbulent* treatment, with a contribution of 9%–24% of the population. Overall, the data indicate that under turbulence, the G2/M phase extended along most of diel cycle, without an arrest in any particular phase. In turbulent conditions, the estimated durations of S and G2/M phases were 2 h 40 min and 9 h 20 min, respectively. Thus, at least after 48 h of exposure to turbulence (on days 9–10 of the experiment), the duration of the S phase was ~19% shorter, and that of the G2/M was ~75% longer than the corresponding periods in the *Still* treatment.

Long-term effects of turbulence in the cell cycle. Exponential phase: The flow cytometric measurements at 0:00 h (obtained once per day until the end of the experiment; Fig. 3, a, c, and e) indicate that, in this period of the diel cycle and during the exponential phase (days 8–12, Fig. 2), most of the *Still* cells (88%–94%) were in G1 phase, while ~2%–10% were in S, and 2%–5% were in G2/M. In the *Turbulent* flasks, considering all the data corresponding to the exponential period (days 8–11, Fig. 2), the population in G1 was significantly lower (Fig. 3a, Table 1), and the cohort in G2/M was significantly higher (Fig. 3e, Table 1), than in the *Still* ones. However, the two treatments did not significantly differ concerning the percentage of the population in S phase (Fig. 3c, Table 1).

In parallel to these general trends during the exponential phase, the *Turbulent* treatments had a significantly higher ($U = 9.0$; $P = 0.000$, $n = 14$) presence of large cells, identified in the range of 25.13–30.17 μm (spherical equivalent diameter) of the size spectra estimated by Coulter Counter (Fig. 4). These large cell numbers correlated well ($r^2 = 0.846$; $P = 0.000$, $n = 14$) with biovolume calculations based on microscopy and the % of cells

TABLE 1. Summary of the main characteristics of the G1, S, and G2/M cell-cycle phases during the 24 h intensive sampling and over the whole experiment.

	G1	S	G2/M
Short-term effects on cell cycle			
Still			
% Population	67–94	2–16	3–32
Daytime	10:30–22:00	19:30–7:30	1:00–12:00
Phase duration		3:20	5:40
Turbulent			
% Population	70–84	3–12	9–24
Daytime	9:00–22:00	16:00–5:00	0:00–11:00
Phase duration		2:40	9:20
Long-term effects on cell cycle			
Exponential phase			
Still % population	88–94	2–10	2–5
Turbulent % population	78–85	4–12	9–17
$n = 18$	$U = 76.0$, $P = 0.001$	$U = 35.0$, $P = 0.657$	$U = 0.0$, $P = 0.000$
Transition phase			
Still % population	95–99	≤5	≤5
Turbulent % population	87–96	≤5	3–12
$n = 20$	$U = 84.0$, $P = 0.010$	$U = 45.0$, $P = 0.703$	$U = 13.0$, $P = 0.005$
Stationary phase			
Still % population	95–99	≤5	≤1
Turbulent % population	95–99	≤1	≤5
$n = 8$	$U = 7$, $P = 0.773$	$U = 12.0$, $P = 0.248$	$U = 1.0$, $P = 0.038$

''% Population'' indicates the range of the population (in %) that contributed to each phase; ''Daytime'' refers to the period of the L:D (local time) cycle when a phase occurs, and its duration (in h) calculated following Carpenter and Chang (1988) is indicated in ''Phase duration.'' In the case of the long-term effects on cell cycle, also indicated are the statistics corresponding to the comparison between *Still* and *Turbulent* treatments, where n indicates the total number of data that are considered, U is the value of the nonparametric Kruskal–Wallis test, and P is its degree of significance.

in G2/M (determined by flow cytometry). This finding suggested that the large cells estimated by the Coulter Counter during the exponential phase corresponded mainly to cells undergoing cell division.

Transition and stationary phases: Along the transition and stationary phases (after days 11 or 12, Fig. 2) and until the end of the experiment, the fraction of the population in G1 phase increased (up to 95%–99%, Fig. 3a) and that in G2/M phase decreased (below the 5%, Fig. 3e) in the two treatments. The percentage of cells in G1 phase was significantly lower in the *Turbulent* cultures than in the *Still* ones, at least until day 17 (transition period, Fig. 3a, Table 1), while the percentage of cells in G2/M was significantly higher in the *Turbulent* than in the *Still* treatments (Fig. 3e, Table 1). Concerning the populations in S phase, there were no significant differences between treatments. During the transition and stationary phases, large cells were also present in all flasks (Fig. 4). However, while the abundance of this size class remained relatively constant in the shaken treatment, it increased notably in the still one after day 14. Microscopic observations revealed that large cells were typical of stationary phase cultures when they did not divide anymore. Toward the end of the experiment, anomalously swollen and bumped cells were also visualized. In the stationary phase, there was no relationship between the abundance of large cells estimated by the Coulter Counter in the 25.13–30.17 μm size fractions and the % of cells in G2/M estimated by flow cytometry ($r^2 = 0.098$).

Mortality: Immediately after the synchronization process (day 7), the abundance of empty and/or broken thecae (7 to 13.05 μm size fraction) was relatively high, especially in the *Still* cultures (Fig. 5). This finding suggested that the synchronization procedure could have somehow affected the cellular viability in part of the population. During the

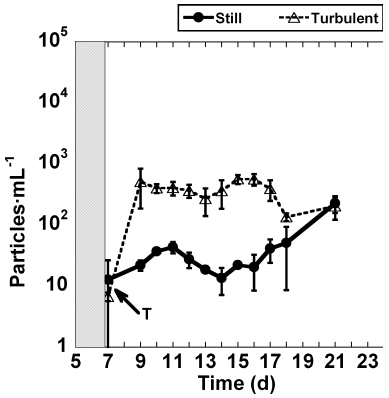

FIG. 4. Temporal changes in the particle abundances estimated in the 25.13 to 30.17 μm size fraction by the Coulter Counter in the *Still* and *Turbulent* treatments. Data points and vertical bars are averages and standard deviations, respectively ($n = 2$). The shaded area represents the synchronization period during days 5 to 7. ''T'' indicates the beginning of turbulence in the corresponding flasks on day 7.

following days of the exponential phase, the proportion of thecae versus vegetative cells decreased markedly in both treatments and reached ~4% on day 11. Thereafter, the contribution of this small-size class in the *Still* flasks decreased slightly and stabilized at ~2% during the rest of the stationary phase. In the *Turbulent* treatment, however, the contribution of the biovolume of broken cells and thecae increased significantly ($U = 5.0$; $P = 0.000$, $n = 32$) until the end of the experiment, likely indicating some degree of cell mortality induced by shaking (Fig. 5).

DISCUSSION

The aim of this study was to evaluate whether turbulence caused mortality and/or alterations of the cell cycle, which could explain the decreased net growth rate and biomass observed previously in *A. minutum* (Berdalet et al. 2007, Bolli et al. 2007) and in different dinoflagellate species subjected to agitation. The two mechanisms could operate simultaneously or separately, depending on different factors. In our present study, shaking for 48 h during the exponential growth period changed both the duration and the diel timing of the cell-cycle phases. In particular, under turbulent conditions, the G2/M phase was longer, and the S phase was shorter and with a smaller fraction of the cell population compared to still conditions. These responses could have caused the lower net growth rate observed under turbulence compared to still treatments. Mortality was not significant during this early phase of the agitation treatment. Nevertheless, when turbulence persisted for >4 d, mortality indicators appeared, coinciding with the entrance of the culture into the stationary phase. Thus, the lower population numbers obtained at the end of the experiment under turbulence would be caused by the combination of an initial alteration of the cell cycle and the subsequent mortality.

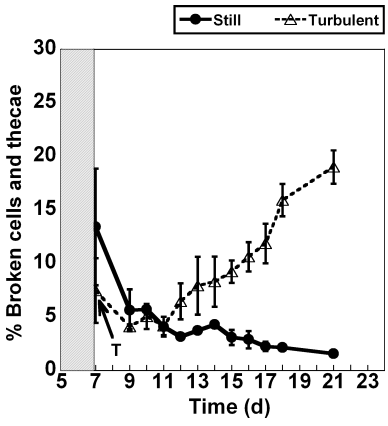

FIG. 5. Temporal changes in the percentage (%) of biovolume estimated in the 7–13.05 μm size fraction with respect to the 13.05–25.13 μm one estimated by Coulter Coulter in the *Still* and *Turbulent* treatments. Data points and vertical bars are averages and standard deviations, respectively ($n = 2$). The shaded area represents the synchronization period during days 5 to 7. "T" indicates the beginning of turbulence in the corresponding flasks on day 7.

The observed elongation of the G2/M phase and the high percentage of the population in this phase of the cell cycle during the 6 d following exposure to turbulence (Fig. 3, c and f), along with the increase of the "large cells" proportion, was interpreted as a transient inhibition of division. This inhibition could have resulted in the slowdown of the division rate and in the up to 2-fold increase in the average cellular DNA content. This finding is consistent with the trends observed in our previous work on *A. minutum* where the low cellular abundances and net growth rates estimated in shaken cultures were accompanied by an average increase in the DNA content per cell up to 1.8 times the value in the still ones (Berdalet et al. 2007). The two studies can be directly compared because the same experimental setup and design were used. Altogether, our results on *A. minutum* agree with the lengthening of the G2 phase in *L. polyedrum* exposed to the continuous low shear generated by a Couette system (Juhl and Latz 2002). However, we did not find the partial arrest in G1 observed by Juhl and Latz (2002) when this species was shaken for 1 to 4 h at low shear stress and also by Yeung and Wong (2003) in *Heterocapsa triquetra* and *Crypthecodinium cohnii* exposed to continuous orbital agitation. As often argued (Berdalet and Estrada 1993, Sullivan et al. 2003), the different results can arise from species-specific responses and from differences in experimental design and setup. Further variations in the methodological approach to estimate effects on the cell cycle can influence the observed responses. For instance, cell-cycle synchronization was used by Yeung and Wong (2003) but not by Juhl and Latz (2002). Intensive sampling is necessary to adequately describe periodic events following the Nyquist-Shannon theory (Platt and Denman 1975). A detailed track of the short-term response to turbulence was performed in the experiments with *A. minutum* (every 2 h over 24 h of an L:D cycle) and with *C. cohnii* (every 2 h over 12 h). Nevertheless, *L. polyedrum* and *H. triquetra* were sampled only once every 12 or 24 h.

The elongation of the G2/M phase observed in *A. minutum* under turbulence can also support, or at least does not invalidate, the hypothesis that turbulence could produce an alteration of the microtubule assemblage during the dinomitosis hypothesized ~20 years ago (Karentz 1987, Berdalet 1992). Mechanical agitation could activate the spindle assembly checkpoint (SAC; Rieder et al. 1995) and delay the completion of the cell cycle. For instance, in *C. cohnii*, nocodazole (Yeung et al. 2000), an antineoplastic agent that interferes with the polimeration of microtubules, induced the

activation of the spindle checkpoint with the subsequent elongation of the G2/M. Sensitivity to mechanical stress is a general cell property (Ingber et al. 1994, Nicklas 1997 and references therein, Gillespie and Walker 2001). Mechanical forces can affect intracellular events directly through the cell surface and cytoskeleton. Unfortunately, the research at this small biological scale is a challenge.

A loss of synchronization of the division process with the diel cycle was a consequence of the elongation of the G2/M phase. Ecologically, it has been argued that a diel-phased division could reduce competition and constitute a selective advantage under grazing pressure (Chisholm et al. 1978, Jansen et al. 2006). Physiologically, the control of division timing could help maintain the order of basic cellular events. Clock-coupled temporal ordering might be selected for stable, predictable environments, whereas less rigid cell-cycle timing would thrive in environments where the population is subjected to widely varying conditions (Chisholm 1981).

In this study, mortality was approached by combining microscopy and Coulter Counter. The different observations provided a rather qualitative indication of mortality, although no rates could be estimated. As already stated, for unknown reasons, cell viability methods (Veldhuis et al. 1997, 2001, Jochem 1999, Garvey et al. 2007) failed to differentiate live and dead cells of *A. minutum* under our experimental conditions in previous tests. Based on our qualitative and indirect approach, the obtained data suggest that cell mortality occurred after 4 d of shaking. Although an elongation of the cell cycle could have repaired potential alterations of the cell division caused by turbulence, the persistence of this stressor could have resulted in a permanent cell-cycle arrest, which in turn could have stimulated the cascade of regulated events that are conducive to cell death (Franklin and Berges 2004). In this sense, turbulence could be considered as a signal inducing cell death (programmed or not), similar to nutritional deprivation, drugs, inhibitors of signaling molecules, oxidative stress, heat shock, aging or differentiation, and mutations in cell-cycle regulating genes described in multicellular organisms (reviewed in Debrabant et al. 2003). In dinoflagellates, depletion of dissolved CO_2 has been reported to induce cell death in both natural and cultured populations of *Peridinium gatunense* (Vardi et al. 1999). Increasing our understanding of the pathways through which turbulence induces cell death can contribute to insights into the mechanisms of programmed cell death in dinoflagellates and in phytoplankton in general.

In the present study, the experimental turbulent energy dissipation rate used was high, although close to the range estimated during stormy turbulent events in the NW Mediterranean, which last for ~4–8 d (Guadayol and Peters 2006). This phenomenon was discussed in our previous studies (Berdalet et al. 2007, Bolli et al. 2007). Interestingly, a modification of the cell cycle was evident after 24 h under turbulence, and it was tracked over the second and third days of exposure to shaking, while mortality appeared after >4 d under turbulence. Further physiological changes had been observed after 12 h of shaking in *A. sanguinea* (Berdalet 1992), after 1–2 d in *P. triestinum* and *A. minutum* (Berdalet et al. 2007), and after 4 d in *A. catenella* (Bolli et al. 2007). Thus, the physiological responses to agitation occurred after a period of time compatible with the duration of natural stormy events. Those results confirm the physiological sensitivity to natural high levels of turbulence of *A. minutum* and, likely, other dinoflagellate species (at least those tested under similar experimental conditions). Sullivan et al. (2003) reported that high concentrations of *A. catenella* occured found as a subsurface bloom in a narrow depth interval (~2 m), where both current shear and turbulence intensity were at a minimum. Those organisms could detect changes in the small-scale hydrodynamics and modulate their migratory behavior (Karp-Boss et al. 2000) for the best positioning in the water column compatible with their division and life cycle. An open field of research is to obtain simultaneous measurements of the hydrodynamics and the distribution of dinoflagellates at spatiotemporal scales compatible with their biological processes.

This work has been supported by the Spanish funded projects TURDITOX (CTM2005-03547/MAR), TURECOTOX (CTM2006-13884-C02-00/MAR) and by the EU project SEED (GOCE-CT-2005-003875). G. Llaveria held an FPU fellowship from the Spanish Ministry of Science and Education (SMSE). R. Figueroa had an I3P postdoctoral contract of the CSIC. E. Garcés's work was supported by a Ramon y Cajal contract of the SMSE. This research is endorsed to the IOC/SCOR program GEOHAB. We appreciate the reviews and suggestions provided by anonymous referees, which improved the quality of our manuscript.

Anderson, D. M. & Lindquist, N. L. 1985. Time-course measurements of phosphorous depletion and cyst formation in the dinoflagellate *Gonyaulax tamarensis*. *J. Exp. Mar. Biol. Ecol.* 86:1–13.

Anderson, D. M., Nosenchuck, D. M., Reynolds, G. T. & Walton, A. J. 1988. Mechanical stimulation of luminescence in the dinoflagellate *Gonyaulax polyedra* Stein. *J. Exp. Mar. Biol. Ecol.* 122:277–88.

Berdalet, E. 1992. Effects of turbulence on the marine dinoflagellate *Gymnodinium nelsonii*. *J. Phycol.* 28:267–72.

Berdalet, E. & Estrada, M. 1993. Effects of turbulence on several phytoplankton species. *In* Shimizu, T. S. Y. [Ed.] *Toxic Phytoplankton Blooms in the Sea.* Developments in Marine Biology, 5th International Conference on Toxic Marine Phytoplankton, Rhode Island, USA. Elsevier, New York, pp. 737–40.

Berdalet, E. & Estrada, M. 2005. Effects of small-scale turbulence on the physiological functioning of marine algae. *In* Durvasula, S. R. [Ed.] *Algal Cultures, Analogues and Applications.* Science Publishers, Enfield, New Hampshire, pp. 459–500.

Berdalet, E., Peters, F., Koumandou, L., Roldán, C., Guadayol, Ò. & Estrada, M. 2007. Species-specific physiological response of dinoflagellates to quantified small-scale turbulence. *J. Phycol.* 43:965–77.

Bolli, L., Llaveria, G., Garcés, E., Guadayol, Ò., van Lenning, K., Peters, F. & Berdalet, E. 2007. Modulation of ecdysal cyst and

toxin dynamics of two *Alexandrium* (Dinophyceae) species under small-scale turbulence. *Biogeosciences* 4:559–67.
Carpenter, E. J. & Chang, J. 1988. Species specific phytoplankton growth rates via diel DNA synthesis cycles. I. Concept of the method. *Mar. Ecol. Prog. Ser.* 43:105–11.
Chen, D., Muda, K., Jones, K., Leftley, J. & Stansby, P. 1998. Effect of shear on growth and motility of *Alexandrium minutum* Halim, a red-tide dinoflagellate. *In* Reguera, B., Blanco, J., Fernández, M. L. & Wyatt, T. [Eds.] *Harmful Algae.* Xunta de Galicia and Intergovernmental Oceanographic Commission of UNESCO, Vigo, Spain, pp. 352–5.
Chisholm, S. W. 1981. Temporal patterns of cell division in unicellular algae. *In* Platt, T. [Ed.] *Physiological Bases of Phytoplankton Ecology. Bull. Can. J. Fish. Aquat. Sci.* 210:150–81.
Chisholm, S. W., Azam, F. & Eppley, R. W. 1978. Silicic acid incorporation in marine diatoms on light:dark cycles: use of an assay for phased cell division. *Limnol. Oceanogr.* 23:518–29.
Debrabant, A., Lee, N., Bertholet, S., Duncan, R. & Nakhasi, H. L. 2003. Programmed cell death in trypanosomatids and other unicellular organisms. *Int. J. Parasitol.* 33:257–67.
Delgado, M., Estrada, M., Camp, J., Fernandez, J. J., Santmarti, M. & Lleti, C. 1990. Development of a toxic *Alexandrium minutum* Halim (Dinophyceae) bloom in the harbour of Sant Charles de la Rapita (Ebro Delta northwestern Mediterranean). *Sci. Mar.* 54:1–7.
Eppley, R. W., Holm-Hansen, O. & Strickland, J. D. H. 1968. Some observations on the vertical migration of dinoflagellates. *J. Phycol.* 4:333–40.
Estrada, M., Alcaraz, M. & Marrasé, C. 1987. Effects of turbulence on the composition of phytoplankton assemblages in marine microcosms. *Mar. Ecol. Prog. Ser.* 38:267–81.
Figueroa, R. I., Bravo, I. & Garcés, E. 2006. The multiple routes of sexuality in *Alexandrium taylori* (Dinophyceae) in culture. *J. Phycol.* 42:1028–39.
Figueroa, R. I., Garcés, E. & Bravo, I. 2007. Comparative study between the life cycles of *Alexandrium tamutum* and *Alexandrium minutum* (Gonyaulacales, Dinophyceae) in culture. *J. Phycol.* 43:1039–53.
Franklin, D. J. & Berges, J. A. 2004. Mortality in cultures of the dinoflagellate *Amphidinium carterae* during culture senescence and darkness. *Proc. R. Soc. Lond. Ser. B* 271:2099–107.
Fritz, L. & Triemer, R. E. 1985. A rapid simple technique utilizing Calcofluor White M2R for the visualization of dinoflagellate thecal plates. *J. Phycol.* 21:662–4.
Galleron, C. 1976. Synchronization of the marine dinoflagellate *Amphydinium carteri* in dense cultures. *J. Phycol.* 12:69–73.
Garvey, M., Moriceau, B. & Passow, U. 2007. Applicability of the FDA assay to determine the viability of marine phytoplankton under different environmental conditions. *Mar. Ecol. Prog. Ser.* 352:17–26.
Gillespie, P. G. & Walker, R. G. 2001. Molecular basis of mechanosensory transduction. *Nature* 413:194–202.
Guadayol, Ò. & Peters, F. 2006. Analysis of wind events in a coastal area: a tool for assessing turbulence variability for studies on plankton. *Sci. Mar.* 70:9–20.
Guillard, R. R. L. 1973. Division rates. *In* Stein, J. R. [Ed.] *Handbook of Phycological Methods. I. Culture Methods and Growth Measurements.* Cambridge University Press, Cambridge, UK, pp. 289–312.
Guillard, R. R. L. & Hargraves, P. E. 1993. *Stichochrysis immobilis* is a diatom, not a chrysophyte. *Phycologia* 32:234–6.
Halim, Y. 1960. *Alexandrium minutum*, n. gen. n. sp. dinoflagellé provocant des ''eaux rouges''. *Vie Milieu* 11:102–5.
Honsell, G., Nichetto, P., Sidari, L. & Tubaro, A. 1995. Toxic dinoflagellates in the Mediterranean Sea. *G. Bot. Ital.* 129:391–403.
Ingber, D. E., Dike, L., Hansen, L., Karp, S., Liley, H., Maniotis, A., McNamee, H., et al. 1994. Cellular tensegrity: exploring how mechanical changes in the cytoskeleton regulate cell growth, migration, and tissue pattern during morphogenesis. *Int. Rev. Cytol.* 150:173–224.
Jansen, S., Riser, C. W., Wassmann, P. & Bathmann, U. 2006. Copepod feeding behaviour and egg production during a dinoflagellate bloom in the North Sea. *Harmful Algae* 5:102–12.
Jochem, F. J. 1999. Dark survival strategies in marine phytoplankton assessed by cytometric measurement of metabolic activity with fluorescein diacetate. *Mar. Biol.* 135:721–8.
Juhl, A. R. & Latz, M. I. 2002. Mechanisms of fluid shear-induced inhibition of population growth in a red-tide dinoflagellate. *J. Phycol.* 38:683–94.
Juhl, A. R., Trainer, V. L. & Latz, M. I. 2001. Effect of fluid shear and irradiance on population growth and cellular toxin content of the dinoflagellate *Alexandrium fundyense*. *Limnol. Oceanogr.* 46:758–64.
Juhl, A. R., Velazquez, V. & Latz, M. I. 2000. Effect of growth conditions on flow-induced inhibition of population growth of a red-tide dinoflagellate. *Limnol. Oceanogr.* 45:905–15.
Karentz, D. 1987. Dinoflagellate cell cycles. *In* Kumar, H. D. [Ed.] *Phycotalk.* Print House Ltd., Maharashtra, India, pp. 377–97.
Karp-Boss, L., Boss, E. & Jumars, P. A. 2000. Motion of dinoflagellates in a simple shear flow. *Limnol. Oceanogr.* 45:1594–602.
Knoechel, R. & Kalff, J. 1978. An in situ study of the productivity and population dynamics of five planktonic diatoms species. *Limnol. Oceanogr.* 23:195–218.
Latz, M. I., Case, J. F. & Gran, R. L. 1994. Excitation of bioluminescence by laminar fluid shear associated with simple Couette flow. *Limnol. Oceanogr.* 39:1424–39.
Latz, M. I. & Rohr, J. 1999. Luminescence response of the red tide dinoflagellate *Lingulodinium polyedrum* to laminar and turbulent flow. *Limnol. Oceanogr.* 44:1423–35.
Margalef, R. 1978. Life-forms of phytoplankton as survival alternatives in an unstable environment. *Oceanol. Acta* 1:493–509.
Margalef, R., Estrada, M. & Blasco, D. 1979. Functional morphology of organisms involved in red tides, as adapted to decaying turbulence. *In* Taylor, D. L. & Seliger, H. H. [Eds.] *Toxic Dinoflagellate Blooms.* Elsevier North Holland, New York, pp. 89–94.
Motulsky, H. 2003. *Prism 4 Statistics Guide: Statistical Analyses for Laboratory and Clinical Researchers.* GraphPad Software Inc., San Diego, California, 150 pp.
Murray, A. & Hunt, T. 1993. *The Cell Cycle: An Introduction.* Oxford University Press, New York, 251 pp.
Nicklas, R. B. 1997. How cells get the right chromosomes. *Science* 275:632–7.
Pan, Y. & Cembella, A. D. 1998. Flow cytometric determination of cell cycles and growth rates of *Prorocentrum* spp. *In* Reguera, B., Blanco, J., Fernandez, M. L. & Wyatt, T. [Eds.] *VIII International Conference on Harmful Algae.* Xunta de Galicia and Intergovernmental Oceanographic Commission of UNESCO, Vigo, Spain, pp. 173–6.
Peperzak, L., Sandee, B., Jonker, R. & Legrand, C. 1998. Measurement of *Prorocentrum micans* growth rate by flow cytometric analisys of the diel DNA cycle. *In* Reguera, B., Blanco, J., Fernandez, M. L. & Wyatt, T. [Eds.] *VIII International Conference on Harmful Algae.* Xunta de Galicia and Intergovernmental Oceanographic Commission of UNESCO, Vigo, Spain, pp. 177–8.
Peters, F. & Marrasé, C. 2000. Effects of turbulence on plankton: an overview of experimental evidence and some theoretical considerations. *Mar. Ecol. Prog. Ser.* 205:291–306.
Platt, T. & Denman, K. L. 1975. Spectral analysis in ecology. *Annu. Rev. Ecol. Syst.* 6:189–210.
Pollingher, U. & Zemel, E. 1981. In situ and experimental evidence of the influence of turbulence on cell division processes of *Peridinium cinctum* forma *westii* (Lemm.) Lefèvre. *Eur. J. Phycol.* 16:281–7.
Rieder, C. L., Cole, R. W., Khodjakov, A. & Sluder, G. 1995. The checkpoint delaying anaphase in response to chromosome monoorientation is mediated by an inhibitory signal produced by unattached kinetochores. *J. Cell Biol.* 130:941–8.
Smayda, T. J. & Reynolds, C. S. 2001. Community assembly in marine phytoplankton: application of recent models to harmful dinoflagellate blooms. *J. Plankton Res.* 23:447–61.

Smith, B. C. & Persson, A. 2005. Synchronization of encystment of *Scrippsiella lachrymosa* (Dinophyta). *J. Appl. Phycol.* 17:317–21.
Sullivan, J. M. & Swift, E. 2003. Effects of small-scale turbulence on net growth rate and size of ten species of marine dinoflagellates. *J. Phycol.* 39:83–94.
Sullivan, J. M., Swift, E., Donaghay, P. L. & Rines, J. E. B. 2003. Small-scale turbulence affects the division rate and morphology of two red-tide dinoflagellates. *Harmful Algae* 2:183–99.
Taroncher-Oldenburg, G., Kulis, D. M. & Anderson, D. M. 1997. Toxin variability during the cell cycle of the dinoflagellate *Alexandrium fundyense*. *Limnol. Oceanogr.* 42:1178–88.
Thomas, W. H. & Gibson, C. H. 1990. Quantified small-scale turbulence inhibits a red tide dinoflagellate, *Gonyaulax polyedra*. *Deep-Sea Res.* 37:1583–93.
Tuttle, R. C. & Loeblich, A. R. 1975. An optimal growth medium for the dinoflagellate *Crypthecodinium cohnii*. *Phycologia* 14:1–8.
Tynan, C. T. 1993. The effects of small scale turbulence on dinoflagellates. PhD dissertation, University of California at San Diego, Scripps Institution of Oceanography, California, 227 pp.
Vardi, A., Berman-Frank, I., Rozenberg, T., Hadas, O., Kaplan, A. & Levine, A. 1999. Programmed cell death of the dinoflagellate *Peridinium gatunense* is mediated by CO_2 limitation and oxidative stress. *Curr. Biol.* 9:1061–4.
Veldhuis, M. J. W., Cucci, T. L. & Sieracki, M. E. 1997. Cellular DNA content of marine phytoplankton using two new fluorochromes: taxonomic and ecological implications. *J. Phycol.* 33:527–41.
Veldhuis, M. J. W., Kraay, G. W. & Timmermans, K. R. 2001. Cell death in phytoplankton: correlation between changes in membrane permeability, photosynthetic activity, pigmentation and growth. *Eur. J. Phycol.* 36:167–77.
Vila, M., Camp, J., Garcés, E., Masó, M. & Delgado, M. 2001. High resolution spatio-temporal detection of potentially harmful dinoflagellates in confined waters of the NW Mediterranean. *J. Plankton Res.* 23:497–514.
White, A. W. 1976. Growth inhibition caused by turbulence in the toxic marine dinoflagellate *Gonyaulax excavata*. *J. Fish. Res. Bd. Can.* 33:2598–602.
Wyatt, T. & Horwood, J. 1973. Model which generates red tides. *Nature* 244:238–40.
Yeung, P. K. K., New, D., Leveson, A., Yam, C., Poon, R. & Wong, J. T. Y. 2000. The spindle checkpoint in the dinoflagellate *Crypthecodinium cohnii*. *Exp. Cell Res.* 254:120–9.
Yeung, P. K. K. & Wong, J. T. Y. 2003. Inhibition of cell proliferation by mechanical agitation involves transient cell cycle arrest at G1 phase in dinoflagellates. *Protoplasma* 200:173–8.
Zirbel, M. J., Veron, F. & Latz, M. I. 2000. The reversible effect of flow on the morphology of *Ceratocorys horrida* (Peridiniales, Dinophyta). *J. Phycol.* 36:46–58.